J Math Chem (2011) 49:1357–1383
DOI 10.1007/s10910-011-9832-5

ORIGINAL PAPER

EPDM accelerated sulfur vulcanization: a kinetic model based on a genetic algorithm

G. Milani · F. Milani

Received: 2 December 2010 / Accepted: 21 April 2011 / Published online: 12 May 2011

Abstract A simple closed form equation for the prediction of crosslinking of EPDM during accelerated sulfur vulcanization is presented. Such a closed form solution is derived from a second order non homogeneous differential equation, deduced from a kinetic model. The kinetic model is based on the assumption that, during vulcanization, a number of partial reactions occurs, both in series and in parallel, which determine the formation of intermediate compounds, including activated and matured polymer. Once written standard first order differential equations for each partial reaction, the differential equation system so obtained is rearranged and, after few considerations, a single second order non homogeneous differential equation with constant coefficients is derived, for which a solution may be found in closed form, provided that the non-homogeneous term is approximated with an exponential function. To estimate numerically the degree of crosslinking, kinetic model constants are evaluated through a simple data fitting, performed on experimental rheometer cure curves. The fitting procedure is a new one, and is achieved using an ad-hoc genetic algorithm, provided that a few points, strictly necessary to estimate model unknown constants with sufficient accuracy, are selected from the whole experimental cure curve. To assess the results obtained with the model proposed, a number of different compounds are analyzed, for which experimental or numerical data are available from the literature. The important cases of moderate and strong reversions are also considered, experiencing a convincing convergence of the analytical model proposed. For the single cases analyzed, partial reaction kinetic constants are also provided.

G. Milani (✉)
Politecnico di Milano, Piazza Leonardo da Vinci 32, 20133 Milano, Italy
e-mail: gabriele.milani@polimi.it

F. Milani
CHEM.CO Consultant, Via J.F. Kennedy 2, 45030 Occhiobello, Rovigo, Italy
e-mail: federico-milani@libero.it

Keywords Sulfur vulcanization · Optimization with GA · Rheometer curves fitting · Second order non homogeneous differential equation

1 Introduction

Sulfur vulcanization is the most practical and popular method for the crosslinking of natural rubber and of the diene synthetic elastomers, such as SBR, butyl, nitrile and EPDM rubbers.

In the most general meaning, vulcanization may be defined as any treatment that decreases the flow of an elastomer, increases its tensile strength and modulus, but preserves its extensibility.

Elemental sulfur is the predominant vulcanizing agent for general-purpose rubbers. It is used in combination with one or more accelerators and an activator system comprising zinc oxide and a fatty acid (normally stearic acid). The most popular accelerators are delayed-action sulphenamides, thiazoles, thiuram sulphides, dithocarbamates and guanidines, etc.

Despite the great diffusion and popularity of such kind of vulcanization process, probably related to the fact that sulfur is the most economical method to vulcanize natural rubber, all the dienic family rubbers and EPDM elastomers, its chemistry of vulcanization is somewhat complex and has not been well understood throughout the century of practice of the process, since its discovery by Goodyear in 1839 [1–3]. Focusing exclusively on EPDM rubber, due the prohibitive complexity of the reactions induced by sulfur during crosslinking—differently to peroxidic curing—no precise reaction kinetic formulas are available in the existing literature. However, for EPDM, the basic reactions involved, see also Fig. 1 for a rough schematization, are commonly accepted [4–15] to be the following:

$$\begin{aligned}
&\text{(a)} \quad P + A \overset{K_1}{\rightarrow} P_1^* \\
&\text{(b)} \quad P_1^* \overset{K_2}{\rightarrow} P_v \\
&\text{(c)} \quad P_v \overset{K_3}{\rightarrow} Q_x \\
&\text{(d)} \quad P_v \overset{K_4}{\rightarrow} D_e \\
&\text{(e)} \quad P_v \overset{K_5}{\rightarrow} P_{v_f}
\end{aligned} \tag{1}$$

Where:

- P and A are the polymer (EPDM) and soluble sulphureted zinc complex (S_8 + accelerators +ZnO + stearic acid) respectively;
- P_1^* is the pendent sulfur (crosslink precursor);
- P_v is the reticulated EPDM;

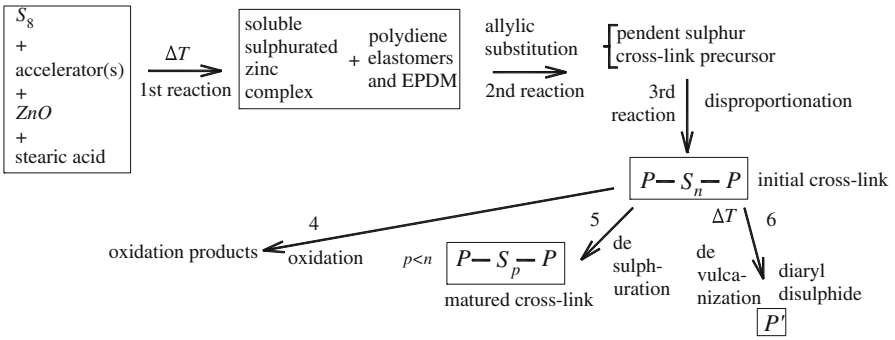

Fig. 1 Products and schematic reaction mechanisms of accelerated sulfur vulcanization of EPDM elastomers

– P_{v_f}, Q_x and D_e are the matured cross-link, the oxidation product and diaryldisulphide respectively;
– $K_{1,\ldots,5}$ are kinetic reaction constants, which depend only on reaction temperature.

Reaction (a) in (1) represents the allylic substitution in Fig. 1, reaction (b) is the disproportionation, whereas reactions (c) (d) and (e) occurring in parallel are respectively the oxidation, the de-sulphuration and the de-vulcanization.

In order to have a precise insight into the sulfur vulcanization kinetic, in absence of standard chemical reaction kinetics available, it is commonly accepted that the rheometer curve (also called cure curve), repeated at different external curing temperatures, is the best way to have a quantitative information on the cross-linking density obtained—[16,17]—at different temperatures and curing time for sulfur vulcanization. The higher is the number of curves collected, the more precise is the database describing the curing behavior at different temperatures of the compound analyzed.

In this context, the aim of the work hereafter presented is to propose a combined analytical-numerical procedure for the interpretation of accelerated sulfur curing, aimed at the prediction of any single intermediate reaction velocity and amount, which bases on the utilization of existing experimental cure curves for a given compound.

To summarize, the analytical-numerical approach proposed relies in the following blocks:

1. For a given rubber compound, existing experimental cure curves are collected from the literature, possibly at different vulcanization temperatures, ranging from low to high. The practical applicability of the model, obviously, would require to perform at least one cure test on the compound at hand, which still remains one of the less expensive laboratory tests that may be required.
2. The analytical-numerical model bases on the assumption that, during vulcanization, the partial reactions shown in (1) occur, both in series and in parallel. They determine the formation of intermediate compounds, including activated and matured polymer. Once known partial reaction constants, a numerical estimation of the degree of crosslinking is possible. From a mathematical point of view, the set of reactions (1) reads as a first order partial differential equation system. After some assemblages, a single second order non homogeneous

differential equation with constant coefficients is derived in the paper, for which a solution may be found in closed form, provided that the non-homogeneous term is approximated with an exponential function.

3. To provide an estimation of the degree of vulcanization of cured EPDM, kinetic model constants are evaluated through a genetic algorithm (GA) [18], fitting numerical data on standard rheometer experimental tests, available from a user defined number of points within the whole set of experimental data. The GA utilized in this paper has been already presented in [18], but is applied here for the first time to a minimization problem with 3 independent variables and in a totally different context. A few points from the whole cure curves are needed to obtain reliable results.

From the above considerations, it is worth noting that the approach here proposed is somewhat different with respect to previously presented models suitable for the analysis of natural rubber (see for example the successful approach due to Ding and Leonov [19]) and rubber cured with peroxides [18,20,21]. While for natural rubber vulcanized with sulphur, reactions at the base of the process are complex and a rather approximate numerical model is proposed in [19], in the latter case, kinetic reaction to consider is a single one, following the Arrhenius law [21]. For EPDM sulfur vulcanization, reaction kinetic is much more intricate and requires an experimental characterization of the compound itself.

The paper is organized as follows: after a concise review of the most important aspects of accelerated sulfur vulcanization and the description of the properties of the cure curve in Sect. 2, the analytical model is derived in Sect. 3. In Sect. 4, the fitting procedure performed through a consolidated GA is outlined and, finally, in Sect. 5 a number of different numerical examples is reported, to fully assess the capabilities of the model proposed.

2 EPDM accelerated sulfur vulcanization

The base for the interpretation of sulfur vulcanization still remains the utilization of experimental cure curves performed on small specimens and obtained both with traditional and rotorless rheometers, see e.g. ASTM D 5289 [22] method.

More in detail, it is commonly accepted that the variation of the cure-meter curve, Fig. 2, intended as the progressive increase of elastic torque during vulcanization, characterizes macroscopically the rubber reticulation level. Cure-meter torque values are here correlated with reticulation kinetic parameters, deduced by a numerical-analytical approach based on the assumption of a sequence of elementary reactions occurring both in series and in parallel, each one represented quantitatively by first order differential kinetic. As mentioned, polymers considered belong all to the family of EPDMs, where it is expected that the mechanism at the base of vulcanization is similar to that generally accepted for polydiene elastomers [23,24].

In the case of EPDM, accelerated sulfur vulcanization results in the substitution of the labile allylic H-atoms by sulfur bridges, yielding alkenyl suphides [9–12].

Pendent ENB unsaturation is not consumed, but actives the allylic positions via a sulfur bridge, yielding cross-link precursors. Subsequently, the actual sulfur

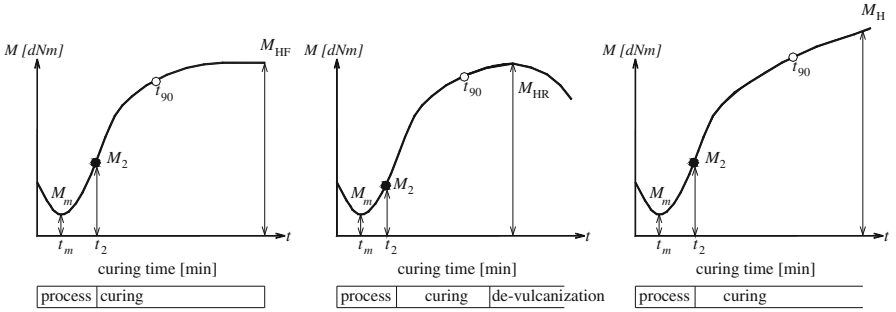

Fig. 2 Typical experimental behavior of a rubber compound during cure meter test

cross-links are formed. Sulfur-substitution of ENB occurs at C-3exo, C-3endo and C-9 (not at bridge head C-1). At elevated temperatures desulfuration occurs, resulting in the formation of shorter sulfur bridges [13]. Side reactions are frequently observed for polydiene elastomers, such as cis-trans isomerization, allylic rearrangement and/or the formation of conjugated dienes and trienes, but do not occur during vulcanization of EPDM containing ENB, because of the stability of the tris-alkyl substituted unsaturation in ENB and its isolation from other ENB units in the macromolecules. In particular, due to the double bond outside the macromolecule chain of the backbone, very high stability both at high temperatures and in presence of oxidant agents is expected. The formation of carbonyls at C-5 and/or C-8 of ENB-EPDM due to oxidation was shown to be linked to accelerated sulfur vulcanization of EPDM [14]. To summarize, considered all the vulcanization issues previously pointed out, the basic reaction scheme represented in Fig. 1 can be adopted. Each single elementary reaction is considered contemporarily to the others and the overall reticulation occurring during vulcanization (matured polymer concentration) is linked to rheometer cure-curves, deriving numerically standard chemical reaction kinetic constants.

3 The kinetic mathematical model proposed

Chemical reactions occurring during sulfur vulcanization reported in (1) obey the following rate equations:

$$\begin{aligned}
\frac{dP}{dt} &= -K_1 A P \\
\frac{dP_v}{dt} &= K_2 P_1^* - K_3 Q_x - K_4 D_e - K_5 P_{v_f} \\
\frac{dQ_x}{dt} &= K_3 P_v \\
\frac{dD_e}{dt} &= K_4 P_v \\
\frac{dP_{v_f}}{dt} &= K_5 P_v
\end{aligned} \tag{2}$$

By means of the so called xyz method, independent variables may be established.

From stoichiometry of the reaction, it can be argued that:

$$\begin{aligned} A &= A_0 - x \\ P &= P_0 - x \\ P_1^* &= x - y = (P_0 - P) - y = (P_0 - P) - \left(P_v + Q_x + D_e + P_{v_f}\right) \\ P_v &= y - z - q - r \\ Q_x &= z \\ D_e &= q \\ P_{v_f} &= r \end{aligned} \tag{3}$$

Obviously, from (3) it can be argued that independent variables are: $P(t)$, $P_v(t)$, $Q_x(t)$, $D_e(t)$, $P_{v_f}(t)$. The aim is to provide an analytical expression for vulcanized rubber, i.e. concentration of $P_v(t)$ with respect to time.

From (2) and (3), the following set of differential equations is deduced:

$$\begin{aligned} \text{(a)}\quad & \frac{dP}{dt} = -K_1 A P \\ \text{(b)}\quad & \frac{dP_v}{dt} = K_2 P_1^* - K_3 Q_x - K_4 D_e - K_5 P_{v_f} \\ & \qquad = K_2 \left[(P_0 - P) - \left(P_v + Q_x + D_e + P_{v_f}\right)\right] \\ & \qquad\quad -K_3 Q_x - K_4 D_e - K_5 P_{v_f} \\ \text{(c)}\quad & \frac{dQ_x}{dt} = K_3 P_v \\ \text{(d)}\quad & \frac{dD_e}{dt} = K_4 P_v \\ \text{(e)}\quad & \frac{dP_{v_f}}{dt} = K_5 P_v \end{aligned} \tag{4}$$

Differentiation of Eq. (4)(b) with respect to time leads to:

$$\begin{aligned} \frac{d^2 P_v}{dt^2} = -K_2 \left(\frac{dP}{dt} + \frac{dP_v}{dt} + \frac{dQ_x}{dt} + \frac{dD_e}{dt} + \frac{dP_{v_f}}{dt}\right) - K_3 \frac{dQ_x}{dt} - K_4 \frac{dD_e}{dt} \\ -K_5 \frac{dP_{v_f}}{dt} \end{aligned} \tag{5}$$

Considering also relations reported in (4), (5) can be re-written as follows:

$$\frac{d^2 P_v}{dt^2} + K_2 \frac{dP_v}{dt} + \widetilde{K}^2 P_v = -K_2 \frac{dP}{dt} = K_1 K_2 A P \tag{6}$$

Having indicated with $\widetilde{K}^2$ the following constant:

$$\widetilde{K}^2 = K_2 (K_3 + K_4 + K_5) + K_3^2 + K_4^2 + K_5^2 \tag{7}$$

Assuming that moles of A are equals to moles of P, as stoichiometry of reaction suggests [15], we can write that:

$$\begin{array}{l} \frac{dP}{dt} = -K_1 A P \\ \frac{dA}{dt} = -K_1 A P \end{array} \tag{8}$$

Hence $P_0 - P = A_0 - A$—see also Eq. (3)—and if $P_0 = A_0$ Eq. (8) becomes:

$$\frac{dP}{dt} = -K_1 P^2 \tag{9}$$

Which is a first order differential equation with separable variables. For (9) the definite integral is:

$$\begin{aligned} -\frac{1}{P(t)} + \frac{1}{P_0} = -K_1 t \Rightarrow P(t) P_0 K_1 t = P_0 - P(t) \\ \Rightarrow P(t) = \frac{P_0}{(P_0 K_1 t + 1)} \end{aligned} \tag{10}$$

Substituting the explicit solution for $P(t)$—Eq. (10)—into (6) we obtain the following differential equation:

$$\frac{d^2 P_v}{dt^2} + K_2 \frac{dP_v}{dt} + \widetilde{K}^2 P_v = -K_2 \frac{dP}{dt} = \frac{K_1 K_2 P_0^2}{(P_0 K_1 t + 1)^2} \tag{11}$$

Which is a not homogeneous second order differential equation with constant coefficients. In order to determine the analytical expression of function $P_v(t)$, the solution of the associated homogeneous differential equations as well as a particular integral must be found.

The determination of integrals of the homogeneous equation corresponding to the left hand side of (11) is trivial and can be achieved considering roots of the characteristic polynomial:

$$\lambda^2 + K_2 \lambda + \widetilde{K}^2 = 0 \tag{12}$$

Which are:

$$\lambda_{1,2} = \frac{-K_2 \pm \sqrt{K_2^2 - 4\widetilde{K}^2}}{2} = \alpha \pm \beta \tag{13}$$

Where $\alpha = -1/2K_2$ and $\beta = \sqrt{(K_2/2)^2 - \widetilde{K}^2}$. From obvious physical considerations, it can be argued that $K_2 >> K_3 \approx K_4 \approx K_5$ and hence $K_2/2 > \widetilde{K}$, meaning that $(K_2/2)^2 - \widetilde{K}^2 > 0$.

In this case, the solution of the homogeneous differential equation corresponding to (6) is:

$$P_v(t) = C_1 e^{(\alpha+\beta)t} + C_2 e^{(\alpha-\beta)t} \tag{14}$$

Where C_1 and C_2 are two constants that can be determined from initial conditions.

The determination of the particular integral of (11) is not an easy task. Indeed, to find a particular integral for function $g(t)$, where:

$$g(t) = \frac{1}{(P_0 K_1 t + 1)^2} \tag{15}$$

may become very tedious.

In absence of consolidate ad-hoc procedures, the so-called general technique of the variation of the arbitrary constants should be utilized. However, such a general procedure provides only first derivatives of some functions entering in the particular integral and their analytical integration is in any case not possible. Here, an alternative procedure is proposed, which consists in substituting the original function $g(t)$, representing (apart multiplying constants) the right hand side of (11) with a fitting function in the following form:

$$f\,(t) = \gamma_1 e^{\gamma_2 K_1 P_o t} \tag{16}$$

Where γ_1 and γ_2 are further constants to be determined in such a way that (16) fits as close as possible (15).

(16) has the rather important advantage that is an exponential function, for which a particular integral is at disposal.

To make (16) near to the original function (15), we require that:

$$\begin{gathered} f\,(0) = g\,(0) \\ \int_0^{t_m \to \infty} f\,(t)\,dt = \int_0^{t_m \to \infty} g\,(t)\,dt \end{gathered} \tag{17}$$

Here it is worth noting that the first request means that functions have the same initial value, whereas the second corresponds to impose that the average decay of not polymerized reagent is the same, with the implicitly accepted simplifying hypothesis that at the end of the test (in practice for an infinite time) the not polymerized reagent is negligible.

From (17) we obtain that:

$$\gamma_1 = 1 - \frac{1}{K_1 P_0} \frac{1}{K_1 P_0 t + 1}\Bigg|_0^\infty = -\frac{1}{\gamma_2 K_1 P_0} e^{-\gamma_2 K_1 P_0 t}\Bigg|_0^\infty \Rightarrow \gamma_2 = 1 \tag{18}$$

From (18), the not homogeneous differential equation (11) can be re-written as follows:

$$\frac{d^2 P_v}{dt^2} + K_2 \frac{dP_v}{dt} + \widetilde{K}^2 P_v = K_1 K_2 P_0^2 e^{-K_1 P_0 t} \tag{19}$$

For (19), the determination of a particular integral is trivial. It is:

$$P_v^p(t) = K_1 K_2 P_0^2 \left[(K_1 P_0)^2 - K_2 (K_1 P_0) + \widetilde{K}^2 \right]^{-1} e^{-K_1 P_0 t} \tag{20}$$

Where $P_v^p(t)$ indicates the particular integral.

Hence, from (19) and (14), the solution of the differential equation is:

$$\begin{aligned} P_v(t) = {} & C_1 e^{(\alpha+\beta)t} + C_2 e^{(\alpha-\beta)t} \\ & + K_1 K_2 P_0^2 \left[(K_1 P_0)^2 - K_2 (K_1 P_0) + \widetilde{K}^2 \right]^{-1} e^{-K_1 P_0 t} \end{aligned} \tag{21}$$

with first derivative:

$$\begin{aligned} \frac{dP_v(t)}{dt} = {} & (\alpha+\beta) C_1 e^{(\alpha+\beta)t} + (\alpha-\beta) C_2 e^{(\alpha-\beta)t} \\ & - K_1^2 K_2 P_0^3 \left[(K_1 P_0)^2 - K_2 (K_1 P_0) + \widetilde{K}^2 \right]^{-1} e^{-K_1 P_0 t} \end{aligned} \tag{22}$$

To fully solve the problem, it is necessary to determine constants C_1 and C_2. They are found from initial conditions:

$$\begin{aligned} & P_v(0) = 0 \\ & \left. \frac{dP_v}{dt} \right|_{t=0} = K_2 P^*(0) = 0 \end{aligned} \tag{23}$$

(23) leads to the following linear system of equations:

$$\begin{cases} C_1 + C_2 = -\rho \\ (\alpha+\beta) C_1 + (\alpha-\beta) C_2 = K_1 P_0 \rho \end{cases} \Rightarrow$$

$$\begin{cases} C_2 = -\rho - C_1 \\ 2\beta C_1 = (K_1 P_0 + \alpha - \beta)\rho \end{cases} \Rightarrow \begin{cases} C_2 = \rho \left(-\frac{K_1 P_0}{2\beta} - \frac{\alpha}{2\beta} - \frac{1}{2} \right) \\ C_1 = \rho \left(\frac{K_1 P_0}{2\beta} + \frac{\alpha}{2\beta} - \frac{1}{2} \right) \end{cases} \tag{24}$$

having defined $\rho = K_1 K_2 P_0^2 \left[(K_1 P_0)^2 - K_2 (K_1 P_0) + \widetilde{K}^2 \right]^{-1}$.

To summarize, the concentration of vulcanized polymer within the mixture during the vulcanization time obeys the following equation:

$$P_v(t) = C_1 e^{(\alpha+\beta)t} + C_2 e^{(\alpha-\beta)t} + \rho e^{-K_1 P_0 t}$$
$$\begin{cases} C_2 = \rho\left(-\frac{K_1 P_0}{2\beta} - \frac{\alpha}{2\beta} - \frac{1}{2}\right) \\ C_1 = \rho\left(\frac{K_1 P_0}{2\beta} + \frac{\alpha}{2\beta} - \frac{1}{2}\right) \\ \rho = K_1 K_2 P_0^2 \left[(K_1 P_0)^2 - K_2 (K_1 P_0) + \widetilde{K}^2\right]^{-1} \\ \alpha = -\frac{K_2}{2} \\ \beta = \sqrt{(K_2/2)^2 - \widetilde{K}^2} \\ \widetilde{K}^2 = K_2 (K_3 + K_4 + K_5) + K_3^2 + K_4^2 + K_5^2 \end{cases} \tag{25}$$

Kinetic constants to determine are only three, i.e. K_1, K_2 and $\widetilde{K}^2$. To find constants using experimental data, torque values are normalized scaling the peak value to P_0 and translating the initial torque to zero, as suggested by Ding and Leonov [19].

To evaluate such constants, a non-linear constrained minimization problem can be written, i.e. it can be required to minimize the sum of absolute differences between experimental and numerical torque on a subset of experimental points, as follows:

$$\min\left(\sum_{i=1}^{N_s} \left|P_1^{\exp}(t_i) - P_1^{num}(t_i)\right|\right)$$
$$\text{subject to} \left\{ \mathrm{K}_1 > 0 \quad \mathrm{K}_2 > 0 \quad \widetilde{\mathrm{K}} > 0 \right. \tag{26}$$

Where N_s is the number of sampled experimental points (abscissa of the i-th point t_i), $P_1^{\exp}(t_i)$ is the normalized experimental torque value at t_i and $P_1^{num}(t_i)$ is the numerical cross-linking density at t_i.

Problem (26) is a typical non linear constrained minimization problem, which is handled numerically in the paper avoiding the utilization of least square routines, but using a standard GA already presented in [18] and briefly recalled in the following section.

4 The genetic algorithm proposed

The evaluation of kinetic constants K_1, K_2 and $\widetilde{K}^2$ for the problem at hand can be easily tackled with standard genetic schemes [25–29], avoiding in this way procedures based on non-linear optimization approaches. In particular, the advantage is represented by the theoretical simplicity of the procedure itself and the robustness and efficiency in terms of time required for the optimization. Authors compared the performance of a standard non linear programming routine to solve the constrained minimization problem (26) to that typical of a GA. It was found that, generally, the time required to solve (26) with a GA was around 0.7 times that required by a non linear programming routine, meaning that the procedure proposed may be favourably used by practitioners interested in a fast evaluation of crosslinking evolution of EPDM

rubber during curing. In general, a GA is a stochastic global search method that mimics the metaphor of natural biological evolution. At a first attempt, see Goldberg [25], the GA algorithm here proposed classically operates on a population of potential solutions applying the principle of survival of the fittest to produce better and better approximations to a solution. At each generation, a new set of approximations is created by the process of selecting individuals according to their level of fitness in the problem domain and breeding them together using operators borrowed from natural genetics. This process leads to the evolution of populations of individuals that are better suited to their environment than the individuals that they were created from.

In particular, the kernel of the GA proposed is a set of standard genetic operations consisting of reproduction, crossover and mutation and non standard procedures, such as zooming and elitist strategy (see [18] for further details on this issue, already tackled by the authors for similar problems). Each individual is represented by admissible reaction constants, i.e. a sequence of individuals i in the form $(K_1^i, K_2^i, \widetilde{K}_i^2)$. Since individuals are stored as a sequence of three real positive numbers, their encoding by means of binary strings results particularly easy. In this way, the genotypes (chromosome values) can be uniquely mapped onto the decision variable (phenotypic) domain. In a standard GA procedure, the use of Gray coding is necessary to avoid a hidden representational bias in conventional binary representation as the Hamming distance between adjacent values is constant (see Holstien [26] and Haupt and Haupt [27]). For standard operators (mutation, crossover, reproduction), a concise description of both the mathematical background and the parameters adopted is reported in what follows (the reader is referred to Goldberg [25] and Haupt and Haupt [27] for details).

The algorithm here used is the same proposed in [18] in another context and can be summarized as follows:

1. Step 0: an admissible initial population $\mathbf{x} = \{x_i : i = 1, \ldots, N_{ind} | x_i \text{ admissible}\}$ is randomly generated at the first iteration;
2. Step 1: x_i fitness $F(x_i)$ is evaluated as $|P_1^{\exp}(t_i) - P_1^{num}(t_i)|$ at fixed $x_i = t_i$;
3. Step 2: two sub groups are created, denoted as $\bar{\mathbf{x}} = \{\bar{x}_i : i = 1, \ldots, N_{elit} | x_i$ admissible$\}$ and $\mathbf{y} = \mathbf{x} - \bar{\mathbf{x}} = \{y_i : i = 1 :, \ldots, N_{ind} - N_{elit}\}$ respectively. $\bar{\mathbf{x}}$ is the group of all the individuals with the N_{elit} (user defined) higher fitness values (zooming strategy).
4. Step 3a: for each $\bar{x}_i$, a random improvement of the individual (in terms of fitness) is tried, by means of two different mutation operators (1^{st} and 2^{nd} type, as described in what follows). The recursive double operation (applied randomly N_{mut} and N_{mut2} times) leads to new individuals generation ($\bar{x}_{iM}$), which overwrite the original $\bar{x}_i$ only if their fitness $F(\bar{x}_{iM})$ is greater than $F(\bar{x}_i)$. At the end of the double loop, a new sub-group $\bar{\mathbf{x}}_M = \{\bar{x}_{iM} : i = 1, \ldots, N_{elit} | \bar{x}_{iM}$ admissible$\}$ is obtained.
5. Step 3b: for each y_i, a mutation loop (only 1^{st} type mutation) is applied randomly N_{mut} times, leading to an improvement of y_i fitness. The new individuals y_{iM} overwrite the original y_i only if their fitness is greater than y_i one (elitist approach). At the end of the double loop, a new sub-group $\mathbf{y}_M = \{y_{iM} : i = 1, \ldots, N_{ind} - N_{elit} | y_{iM}$ admissible$\}$ is obtained. A classic reproduction operator is applied only for individuals of $\mathbf{y}_M$ with high fitness

(i.e. on $(N_{ind} - N_{elit})/\rho$ parents with user defined parameter $\rho > 1$) in order to create a new offspring group **c**. The remaining $(1 - \rho)(N_{ind} - N_{elit})/\rho$ individuals are generated *ex-novo* using Step 0 procedure and are catalogued into $\mathbf{c}_N = \{c_{Nj} : j : 1, \ldots, (N_{ind} - N_{elit})/\rho | c_{Nj}$ admissible$\}$.

6. Step 4: the final population at the i-th iteration is collected into $\mathbf{x} = [\bar{\mathbf{x}}_M \ \mathbf{c} \ \mathbf{c}_N]$ and the procedure is repeated *ad libitum* from Step 1.

The implementation of non-standard strategies (zooming with elitist strategy) is not necessary in this case, but speeds up the convergence of the fitting in presence of a few fitting points. Authors experienced a reduction of processing time within the range 0.05–0.15 of the time needed for the optimization by a standard GA.

4.1 Generation of admissible individuals

The generation of admissible individuals occurs by means of random processes respecting all admissibility conditions ($K_1 > 0, K_2 > 0$ and $\widetilde{K} > 0$). Such a procedure is followed at the first iteration (for all the N_{ind} individuals) and at each iteration $i > 1$ for $(\rho - 1)(N_{ind} - N_{elit})/\rho$ individuals. A binary representation with chromosomes is used for each individual in the population. If, as is the case here treated, the number of optimization variables (here denoted as N_{var}) is 3 (three are the kinetic variables to optimize) each individual is represented by $N_{bit} = N^1_{bit} + N^2_{bit} + N^3_{bit}$ chromosomes.

As a consequence, the population has N_{bit} chromosomes and is an $N_{ind}xN_{bit}$ matrix filled with random ones and zeros generated using the well known following syntax [27]:

$$\text{pop} = \text{round}(\text{rand}(N_{ind}, N_{bit})) \tag{27}$$

where the function rand(N_{ind},N_{bit}) generates a $N_{ind}xN_{bit}$ matrix of uniform random numbers between zero and one. The function round rounds the numbers to the closest integer which in this case is either 0 or 1. Each row in the pop matrix is obviously an individual encoded with chromosomes. The chromosomes correspond to discrete values of the input variables. In order to pass from a binary representation to a continuous representation, a so called quantization error is introduced. An increase in the number of bits reduces the quantization error.

4.2 Reproduction

Reproduction is applied to $\mathbf{y} = \{y_i : i = 1 : N_{ind} - N_{elit}\}$ group. As usual, for each individual, a fitness value derived from its raw performance measure given by the objective function is assigned. This value is used in the selection to bias towards more fit individuals. Highly fit individuals, relatively to the whole population, have a high probability of being selected for mating whereas less fit individuals have a correspondingly low probability of being selected.

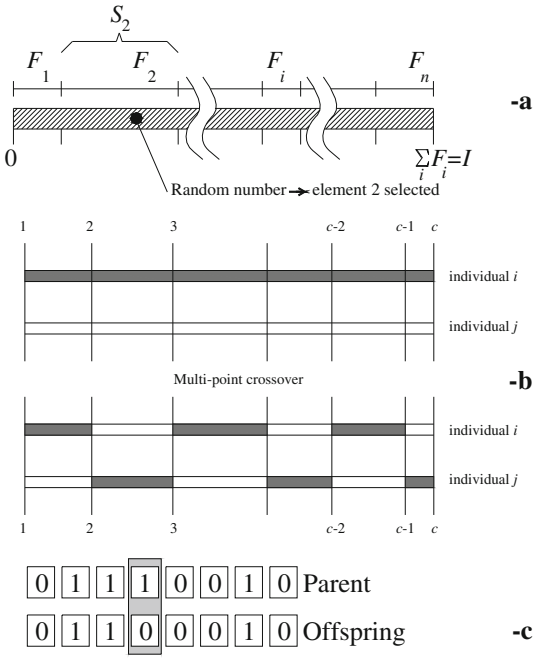

Fig. 3 Selection operation—roulette wheel—(-a), crossover (-b), mutation (-c)

Once that a fitness value is assigned to the individuals, they can be chosen from the population, with a probability according to their relative fitness, and recombined to produce the next generation.

A stochastic sampling with replacement (roulette wheel) is used in the paper. An interval I is determined as the sum of the fitness values F_i of all the individuals in the current population, i.e. $I = \sum F_i$. For each individual i, a sub-interval S_i corresponding to its fitness value in the interval $\left[0\ I\right]$ is determined, i.e $S_i = F_i$, so that $I = \sum S_i$ and the size of the interval associated to each individual is proportional to its fitness, i.e. so that a big sub-interval corresponds to a highly fit individual. To select an individual, a random number is generated in the interval $\left[0\ I\right]$ and the individual whose segment sub-interval spans the random number is selected, see Fig. 3a. This process is repeated until the desired number of individuals have been selected.

Reproduction is active only on **y** sub-population. Only an offspring per pair is generated and a total number of $(N_{ind} - N_{elit})/\rho$ of reproductions is allowed. The remaining $(\rho - 1)(N_{ind} - N_{elit})/\rho$ individuals are generated *ex-novo*. This procedure, which mimics the biological behaviour of an open population, assures a stochastic possibility of introduction of new chromosomes (i.e. individuals) with good characteristics in terms of fitness.

4.3 Zooming

The application of an *ad hoc* technique for the problem at hand is designed to obtain improved results in terms of best fitness at each iteration. The algorithm relies in sub-dividing the initial population into two groups:

$$\bar{\mathbf{x}} = \{\bar{x}_i : i = 1, \ldots, N_{elit} | x_i \text{ admissible}\}$$
$$\mathbf{y} = \mathbf{x} - \bar{\mathbf{x}} = \{y_i : i = 1 :, \ldots, N_{ind} - N_{elit}\} \quad (28)$$

Zooming consists in collecting at each iteration the individuals with higher fitness into an "elite" sub-population $\bar{\mathbf{x}}$ (with user defined dimension N_{elit}). Then, for each individual belonging to the elite, only mutation (with high probability) is applied in order to improve individuals fitness. Two different mutation algorithms are utilized, differing only on the number of cells of each individual involved by the mutation process.

Subsequently, an elitist strategy preserves the original individual if mutation results in a reduction of individual fitness, whereas zooming technique restricts search domain, so improving in any case convergence rate. From a practical point of view, zooming is set by means of the so called zooming percentage $z_{\%}$, defined as the percentage ratio between $\mathbf{x}$ initial population and $\bar{\mathbf{x}}$ sub-population dimension, i.e.:

$$z_{\%} = \frac{N_{elit}}{N_{ind}} 100 \quad (29)$$

4.4 Crossover and mutation

During a generation of a new individual from two parents, a crossover operator is used to exchange genetic information between pairs.

In the present study, we use a multi-point crossover operator, which works as follows: $k_i = \left[1\ 2 \ldots c - 1 \right]$ crossover points are randomly selected on two individuals (parents) represented by c chromosomes (bits), as shown in Fig. 3b. Bits between the crossover points are exchanged between the parents in order to produce a new offspring.

Mutation is applied with high probability directly on existing individuals. Two types of mutation are used (here denoted as 1st and 2nd type).

4.4.1 First type mutation

Such operator is the classic mutation and is applied both on $\bar{\mathbf{x}}$ and $\mathbf{y}$ individuals. For each individual $\bar{\mathbf{x}}_i$ (or $\mathbf{y}_i$) it works stochastically on all the chromosomes (i.e. changing at random one of the individual columns from 1 to N_{bit}), Fig. 3c. The procedure is repeated once on N_{mut} different individuals. Obviously, first type mutation results in a new individual in which only one of the optimization independent variables, after chromosomes decoding, results changed with respect to the original individual.

4.4.2 Second type mutation

Second type mutation is applied only to $\bar{\mathbf{x}}$ individuals, in order to obtain a further improvement of their fitness. It works analogously to the first type algorithm, with the only difference that it changes, for the individual subjected to mutation, a chromosome belonging to K_1, K_2 and $\widetilde{K}$ respectively. Thus, the resulting individual after

chromosomes decoding is different from the original one for all the kinetic constants. The procedure is repeated on N_{mut2} individuals.

Both N_{mut} first type mutations and N_{mut2} second type mutations are user defined.

The final result of the application of both first and second type mutation is a new admissible individual $\bar{x}_{iM}$ with different fitness with respect to $\bar{x}_i$. If $\bar{x}_{iM}$ fitness is higher than that of the original individual (note that the check is executed at each N_{mut} iteration), we overwrite $\bar{x}_i$ with $\bar{x}_{iM}$. All the fitting procedure is handled within the Matlab software [30] by means of non standard routines implemented at this aim by the authors.

5 Comparison between one differential equation model and experimental data

In order to assess the capabilities of the combined GA-differential equation model proposed in reproducing experimental EPDM vulcanization process, several experimental data available in the literature are here re-considered as reference.

To perform a numerical optimization of the kinetic model proposed, experimental cure values are normalized dividing each point of the curve by the maximum torque values, so that experimental data are always within the range 0–1.

Three sets of different data are considered: the first refers to two EPDM commercial products (Dutral by polimeri Europa) at different temperatures (experimental data are available in [7]), the second set is a collection of Sartomer products (with different amounts of several accelerator co-agents, experimental data are collected from [8,17]), whereas the last set consists in two numerical cure curves available in [7] and referred to a commercial ter-polymer tested at 160 and 200 °C.

5.1 First set: Dutral experimental data at different temperatures

Two different EPDMs are considered here. Experimental data are available in [7] and the reader is referred there for a precise experimental characterization of the compounds. Here, it is worth noting that their characteristics, in terms of Mooney viscosity and compositions are summarized in Table 1.

For all types of EPDM, the same formulation was used, with the precise aim of comparing the polymeric matrix in presence of different Mooney viscosity, different

Table 1 First set of numerical simulations (Dutral Ter 4049 and 9046 data): rubber composition

Type of EPDM by Polimeri Europa	Dutral 4044 reference commercial composition	Dutral 4049	Dutral 9046
% Propylene by wt	35	40	31
% ENB by wt	4.0	4.5	9.0
ML (1+4) 100 °C	44	–	67
ML (1+4) 125 °C	–	76	–

Table 2 First set of numerical simulations. Compounds formulation adopted (in phr)

Ingredients	Description	phr
Polymer	Dutral 4044;4049 and 9046	100
Zinc oxide	Activator	5
Stearic acid	Co-agent	1
HAFN 330	Carbon black	80
Paraffinic oil	Wax	50
Sulfur	Vulcanization agent	1.5
TMTD	Tetramethylthiuram disulfide	1.0
MBT	Mercaptobenzothiazole	0.5

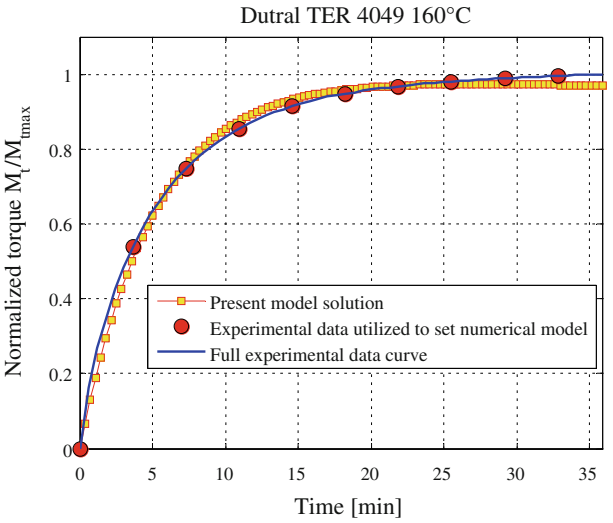

Fig. 4 Dutral TER 4049 160 °C. Comparison between experimental data and the numerical models proposed

ENB content but with a composition where the elastomers are completely in amorphous status. In Table 2, compounds formulation adopted (in phr) is summarized. Each sample was analyzed using a rotor-less cure-meter, following specifics provided for RPA 2000 [22].

Experimental cure curves are available from the literature, see [7], at three different temperatures (160, 180 and 200 °C) for Dutral 4049 and at two different temperatures (160 and 180 °C) for Dutral 9046.

In Fig. 4, a comparison between cure curves provided by the present approach and experimental results is sketched for Dutral TER 4049, for a temperature equal to 160 °C. Dots represent the few points utilized to fit the analytical model using the GA proposed, see problem (26). The typical convergence of the GA approach proposed in reported in Fig. 5. Comparisons for temperatures at 180 and 200 °C are replicated in Figs. 6 and 7 respectively. Again, the agreement with experimental response seems

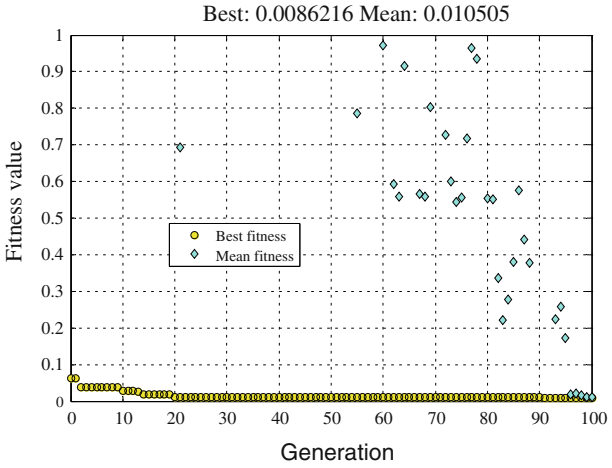

Fig. 5 Dutral TER 4049 160 °C. GA convergence

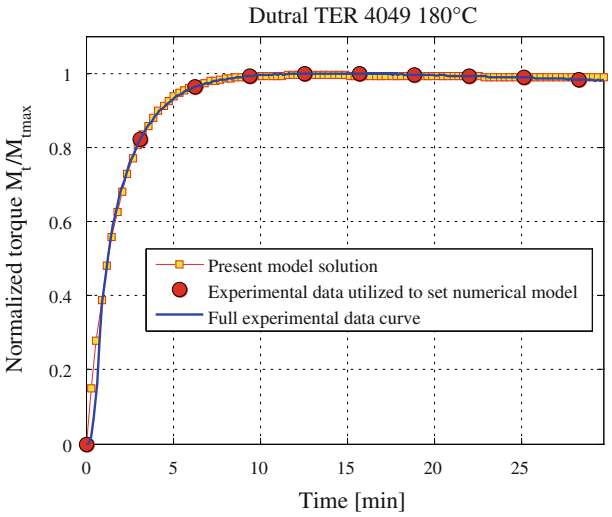

Fig. 6 Dutral TER 4049 180 °C. Comparison between experimental data and the numerical models proposed

rather promising, also in consideration that very few experimental points are needed to obtain a rather satisfactory reproduction of the actual experimental curve.

The same comparisons performed for Dutral TER 4049 are repeated for Dutral TER 9046 in Figs. 8 and 9 respectively at 160 and 180 °C. Also in this case, the reliability of the numerical model proposed seems promising, providing results again in very satisfactory agreement with experimental data. However, for both compounds, the reversion is limited and a full comparison in presence of anomalous behaviors during vulcanization (de-vulcanization) is needed to fully assess the capabilities of the model.

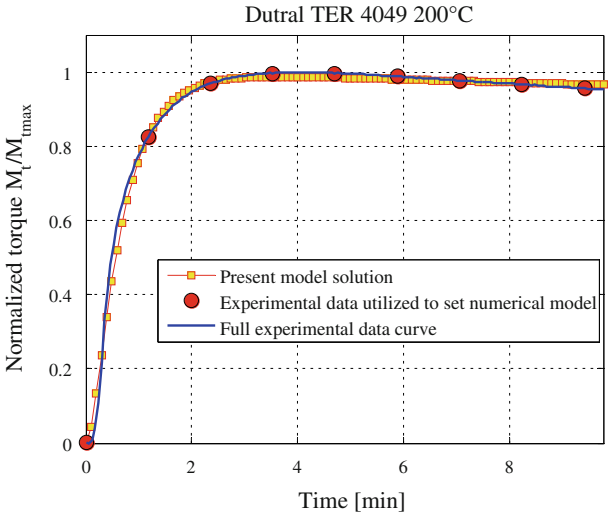

Fig. 7 Dutral TER 4049 200 °C. Comparison between experimental data and the analytical second order differential equation model

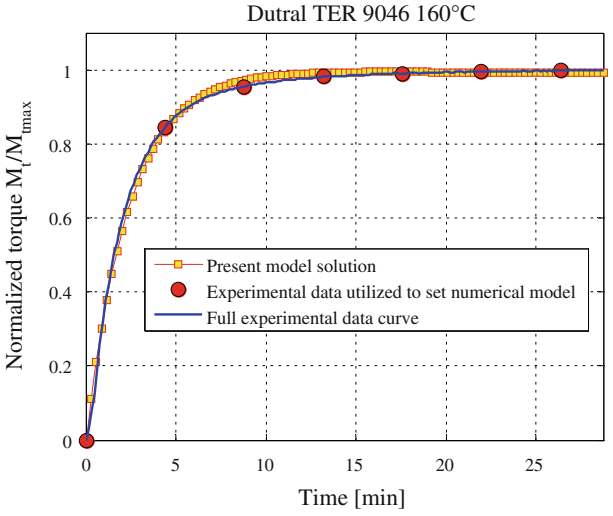

Fig. 8 Dutral TER 9046 160 °C. Comparison between experimental data and the analytical second order differential equation model

5.2 Second set: Sartomer experimental data at different co-agents compositions

Four experimental cure curves collected from Henning [17] are hereafter considered. Experimental cure curves correspond to four different compounds in which different zinc salts are used as activators, namely 5.0 phr zinc oxide, 12.8 phr ZDA, 14.5 phr ZDMA, 10.4 phr ZMMA at molar equivalency. Rubber used is Goodyear Natsyn 2200 ® and the reader is referred to Henning [17] for a detailed description

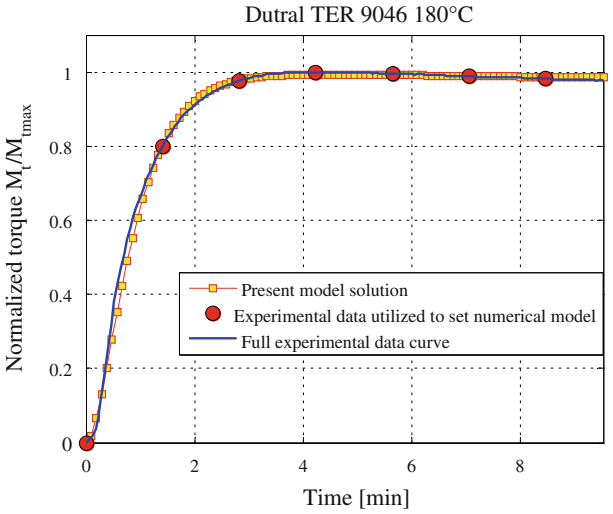

Fig. 9 Dutral TER 9046 180 °C. Comparison between experimental data and the analytical second order differential equation model

Table 3 Second set of numerical simulations (Sartomer data): rubber composition

Ingredient	phr
Natsyn 2200 Goodyear [Polyisoprene (cis-1.4)]	100
N330 Carbon black cabot vulcan 1345	50
Processing oil [Sunoco sunpar 2280]	10
ZnO	variable
Stearic Acid	2
ZDMA (Sartomer SR708) [Zinc dimethacrylate]	variable
Atioxidant-uniroyal chemical naugard Q (TMQ)	1
TBBS [N-t-butylbenzothiazole-2-sulphenamide]	0.7
Sulphur	2.5

of the compound. The exact composition of the blends analyzed is summarized in Table 3.

ZDA indicates a zinc diacrylate produced by Sartomer (Sartomer SR705), ZDMA is a zinc di-metacrylate (Sartomer SR708), whereas ZMMA is a zinc mono-metacrylathe (Sartomer SR709).

Experimental cure curves are obtained at 160° following ASTMD 2084 [4], using an arc deflection of 3°. From Figs. 10 to 13, a full comparison between experimental data provided using the four activators analyzed and the numerical-analytical approximation here proposed is represented. As it is possible to notice, again for all the cases analyzed a very good agreement is found, with also a satisfactory response in the reversion range, especially in the second and last example.

As second set of examples to validate the analytical-numerical model in presence of a marked reversion, we analyze again a Goodyear Natsyn 2200 ® compound

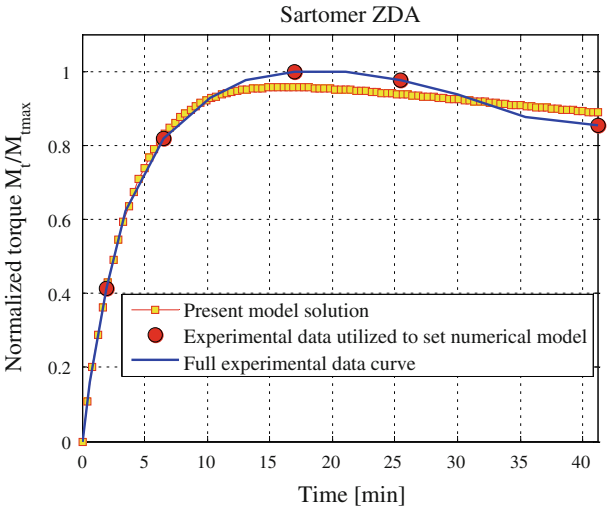

Fig. 10 Sartomer ZDA. Comparison between experimental data and the analytical second order differential equation model

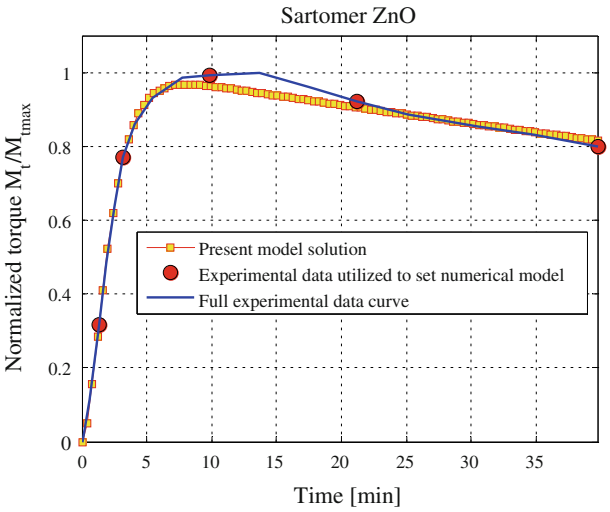

Fig. 11 Sartomer ZnO. Comparison between experimental data and the analytical second order differential equation model

vulcanized exclusively with ZDMA (except for one case, where ZnO has been used) at decreasing concentrations of ZDMA accelerator. Full experimental cure curves are again available from the literature [17] and some of them exhibit reversion. In particular, it is interesting to notice that a reduction of the accelerator concentration in the compound, results in an increase of reversion, which becomes quite predominant at small concentrations of the accelerator. This is a common issue of sulfur vulcanization and is well documented in the literature [31,32]. A full comparison between

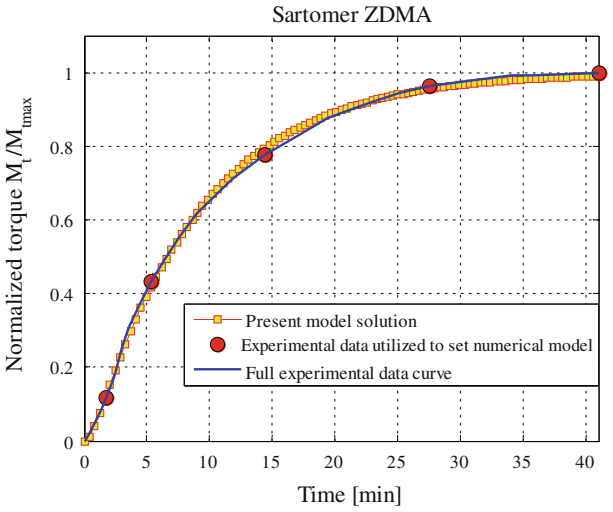

Fig. 12 Sartomer ZDMA. Comparison between experimental data and the analytical second order differential equation model

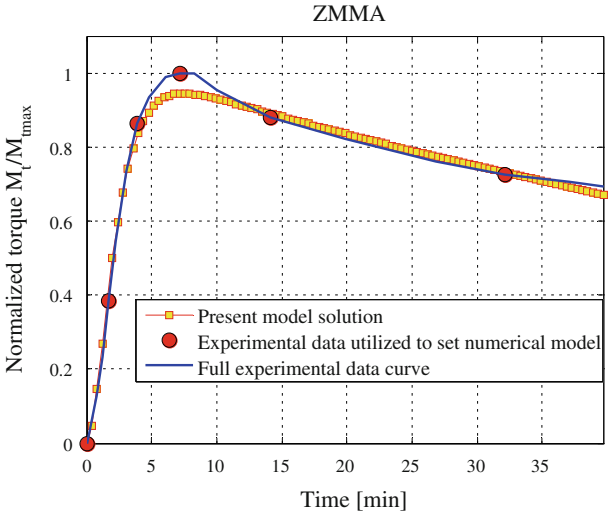

Fig. 13 Sartomer ZMMA. Comparison between experimental data and the analytical second order differential equation model

experimental cure curves and present numerical predictions is provided in Figs. 14, 15, 16, 17. Again, a rather close fitting is obtained, in presence also to severe reversion, especially in the last case (ZDMA 1.81 phr), where an high de-vulcanization occurs (around 50% at the end of the curing process).

From simulations results, it is particularly evident that the numerical model proposed may furnish a quantitative information of reversion at a fixed compound, suitable to establish the most indicated production parameters to use. This could allow to reduce

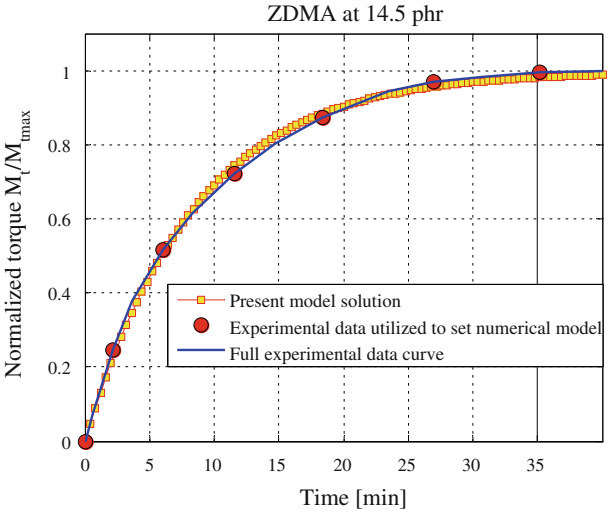

Fig. 14 Sartomer ZDMA at 14.5 phr. Comparison between experimental data and the analytical second order differential equation model

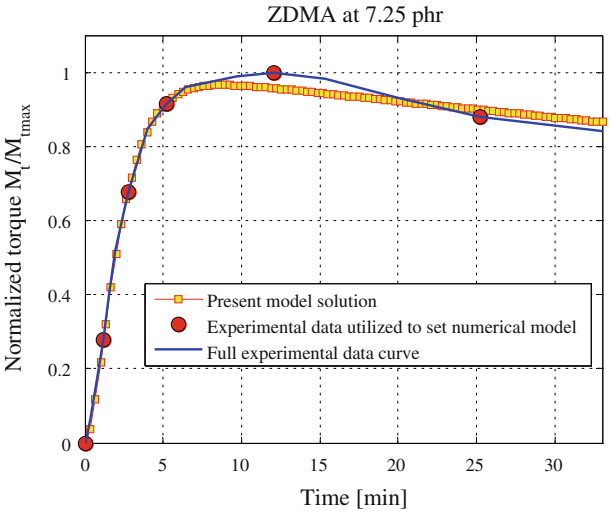

Fig. 15 Sartomer ZDMA at 7.25 phr. Comparison between experimental data and the analytical second order differential equation model

economic losses of real production plants, which usually are designed following simple rule of thumbs.

Nevertheless, it is worth underlining that, in order to predict correctly input parameters to optimize the vulcanization of thick items, it is necessary to have at disposal cure curves of the same compound at different temperatures. Such curves (or only a few meaningful points) may be easily collected in a database and fitted numerically with the procedure proposed.

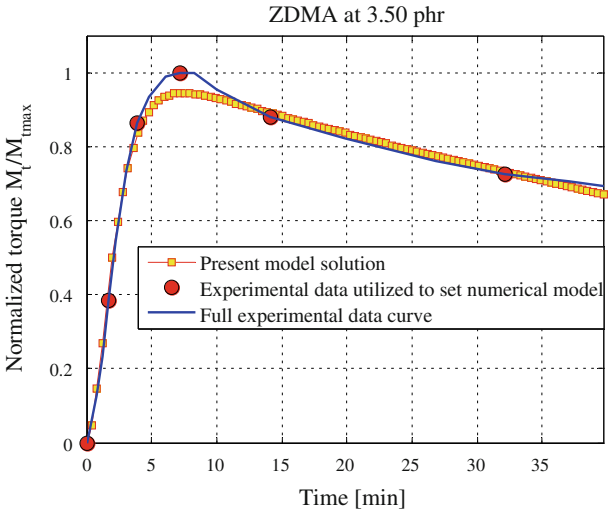

Fig. 16 Sartomer ZDMA at 3.50 phr. Comparison between experimental data and the analytical second order differential equation model

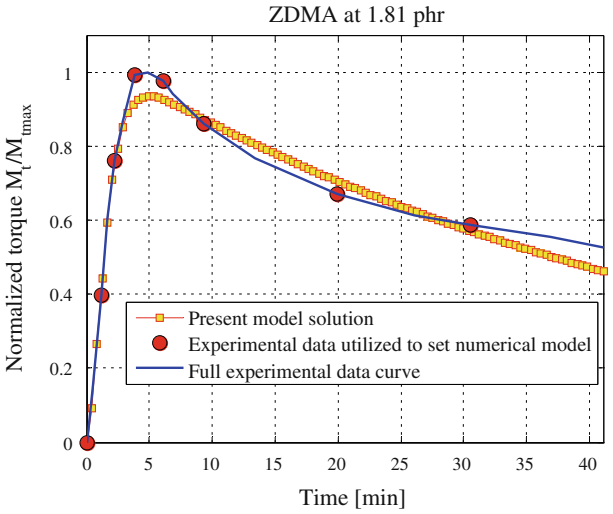

Fig. 17 Sartomer ZDMA at 1.81 phr. Comparison between experimental data and the analytical second order differential equation model

5.3 Third set: Dutral 4334 numerical data

Two numerical cure curves at two different temperatures are available from the literature [7], regarding and EPDM compound (Dutral 4334 by Polimeri Europa) exhibiting reversion. Here it is worth noting that such curves are purely analytical fitting functions (a parabola and two hyperbola) on existing few experimental points and no kinetic

Table 4 Third set of numerical simulations (Dutral TER 4334). Cure curve properties at two different imposed temperatures

Temperature T	160 °C	200 °C
Minimum torque	15 dNm	7 dNm
Scorch torque	20 dNm	12 dNm
t_2- scorch time	150 s	50 s
t_{90}-torque	58 dNm	52 dNm
t_{90}-90% vulcanization time	700 s	200 s
de vulcanization torque	60 dNm	54 dNm
de vulcanization time	2800 s	900 s

considerations are available in [7]. Therefore, the procedure here proposed seems much more powerful with respect to those presented in the recent literature, e.g. [8] and [19]. The compound under consideration has the following percentage composition: propylene 27%, paraffinic oil 30%, ENB 4.5%. The experimental formulation is the following: 140 phr of polymer, 115 phr of filler carbon black (N330), 3 phr of zinc oxide, 2.5 phr of stearic acid, 1.2 phr of 2-mercaptobenzothiazole, 0.8 phr of tetramethylthiuram disulfide, 1.8 of zinc dibutyldithiocarbamide and 2 phr of sulphur. The Mooney viscosity of the compound at 100 °C was equal to 90. The experimental characteristic times (t_2: scorch, t_{90}: 90% vulcanization time, etc.) available from [7], along with the corresponding torque at the different temperatures inspected are summarized in Table 4. The vulcanization characteristics of vulcanizable rubber compounds is experimentally determined by means of a rotor-less cure-meter (ASTM D 5289 [22]). Cure curves are obtained at two different temperatures, namely 160 and 200 °C.

From data collected in Table 4 and the numerical curves provided in [7], the mathematical approximations of the cure curves reported in Figs. 18 (160 °C) and 19 (200 °C) have been obtained with the model proposed.

Again, the agreement is very satisfactory and confirms the effectiveness and the easiness of application of the model proposed.

Finally, for the sake of completeness, a synopsis of reaction kinetic constants found by the combined application of the second order differential equation proposed and the GA fitting procedure presented (solution of problem (26)) is reported in Table 5. Here, it is worth noting only that the dependence of kinetic constants with respect to vulcanization temperature could be studied only for the first sub-set of polymers, for which cure curves at three increasing temperatures are provided. In any case, such study could be performed only a-priori assuming a low of variability for the kinetic constants with respect to temperature. While the most natural choice would be the utilization of the Arrhenius equations, this would be a rather arbitrary assumption and, at present, it is far to be demonstrated that partial reactions follow an exponential law. For this reason, a detailed experimental campaign on a single EPDM blend is needed to fully resolve this issue.

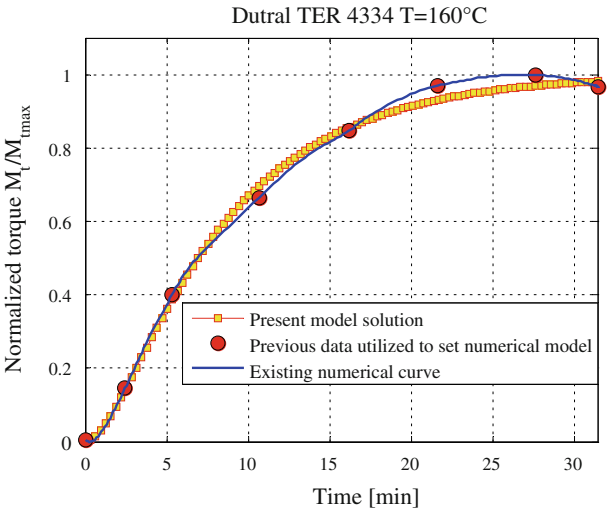

Fig. 18 Dutral TER 4334 160 °C. Comparison between experimental data and the analytical second order differential equation model

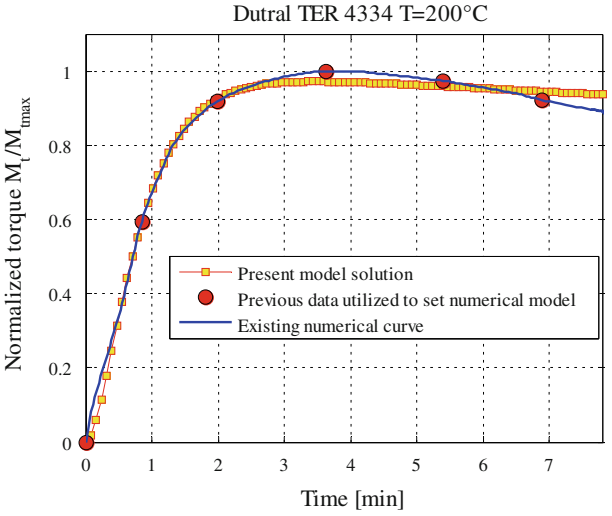

Fig. 19 Dutral TER 4334 200 °C. Comparison between experimental data and the analytical second order differential equation model

6 Concluding remarks

A simple mathematical kinetic model for the interpretation of EPDM sulfur vulcanization has been presented. The model bases on consolidated partial reactions occurring during rubber crosslinking, which lead, from a mathematical point of view, to write a first order differential equation system. After suitable non-standard arrangements, a simple second order non-homogeneous differential equation with constant coefficients

Table 5 Kinetic constants found with the mathematical model proposed

	K_1 [1/mol min]	K_2 [1/min]	$\widetilde{K}$ [1/min]
DutralTer 4049			
T = 160 °C	0.1947	9.89	0.0836
T = 180 °C	0.5518	9.84	0.0673
T = 200 °C	1.7665	6.5034	0.1610
DutralTer 9046			
T = 160 °C	0.4155	9.91	0.067
T= 180 °C	1.7305	2.7847	0.0727
SartomerPDiene			
ZDA	0.2868	9.97	0.1726
ZnO	0.9963	0.7883	0.0664
ZDMA	0.1151	1.6631	6.166×10^{-4}
ZMMA	0.8822	0.8143	0.0941
ZDMA 14.5 phr	0.1261	1.6602	7.013×10^{-4}
ZDMA 7.25 phr	0.6389	1.2481	0.0776
ZDMA 3.50 phr	0.8822	0.8143	0.0941
ZDMA 1.81 phr	1.2918	1.1584	0.1511
DutralTer 4334			
T = 160 °C	0.1352	0.6105	3.067×10^{-4}
T = 200 °C	1.5478	4.4602	0.2214

has been derived, representing the degree of crosslinking at successive instants. The homogeneous associated differential equation may be solved in closed form, whereas the particular root is found substituting the inhomogeneous term with an equivalent (from an integral point of view) function, which may be integrated analytically. A few experimental points are needed to evaluate the constants entering the differential equation (they are only three, namely three partial reaction constants). To fit analytical model constants, existing literature has been used and, in particular, scaled experimental cure curves have been considered. The fitting procedure has been performed on a very limited number of fitting points, leading to a constrained non-linear minimization problem, which has been solved utilizing an existing meta-heuristic GA approach. Several cases of practical interest on three different sets of EPDM and Polyisoprene compounds have been considered to assess the capabilities of the model proposed. In all the cases analyzed, very good agreement with experimental (numerical for the last set) data has been found, especially in presence of moderate and severe reversion (second set of examples).

From simulations results, it can be concluded that the model represents a robust analytical base to predict theoretically kinetic vulcanization parameters as a function of curing temperature, as well as to estimate curing times for the vulcanization of real rubber items, in case of homogeneous temperature distributions from the skin

to the core. Furthermore, the model may allow, at least in principle, to perform an optimization of curing temperatures and exposition times in real production lines.

References

1. C. Goodyear, US Patent 3633 (1844)
2. F.W. Billmeier Jr., *Textbook of Polymer Science*, 3rd edn. (Wiley, London, 1984)
3. M.L. Krejsa, J.L. Koenig, Rubber Chem. Technol. **66**, 376 (1993)
4. A.Y. Coran, Vulcanization, Chap. 7, in *Science and Technology of Rubber*, ed. by R. Frederick Eirich (Academic Press, New York, 1978)
5. L. Bateman (ed.), *The Chemistry and Physics of Rubber-like Substances* (MacLaren, London, 1963)
6. M. Morton (ed.), *Rubber Technology*, 2nd edn. (Van Nostrand Reinhold, New York, 1981)
7. G. Milani, F. Milani. *Experimental Characterization of EPDM Rubber Compounds Through a RPA 2000 Cure-meter*. Chem.Co. Internal report 2010-10.1 (2010)
8. G. Milani, F. Milani, J. Math. Chem. **48**, 530–557 (2010)
9. H.G. Dikland, M. Van Duin, Cross-linking of EPDM studied with optical spectroscopy, in *Spectroscopy of Rubber and Rubbery Materials,* ed. by V.M. Litvinov, P. De (Rapra Technology Ltd., UK, 2002)
10. J.F.M. Van Den Berg, J.W. Beulen, E.F.J. Duynstee, H.L. Nelissen, Rubber Chem. Technol. **57**, 265 (1984)
11. J.F.M. Van Den Berg, J.W. Beulen, J.M.H. Hacking, E.F.J. Duynstee, Rubber Chem. Technol. **57**, 725 (1984)
12. E.F.J. Duynstee, Kautsch. Gummi Kunstst. **40**, 205 (1987)
13. H.K. Frensdorf, Rubber Chem. Technol. **45**, 1348 (1972)
14. R. Winters, W. Heinen, M.A.L. Verbruggen, M. Van Duin, H.J.M. de Groot, Macromolecules **35**(5), 1958–1966 (2002)
15. M. Van Duin, Kautsch. Gummi Kunstst. **55**(4), 205 (2002)
16. B.T. Poh, K.W. Wong, J. Appl. Polym. Sci. **69**, 1301–1305 (1998)
17. S.K. Henning, The use of coagents in sulfur vulcanization: functional zinc salts, in *Proceedings of Spring 167th Technical Meeting of the Rubber Division*, American Chemical Society, San Antonio, TX, 16–18 May 2005
18. G. Milani, F. Milani, J. Math. Chem. **47**, 229–267 (2010)
19. R. Ding, I. Leonov, J. Appl. Polym. Sci. **61**, 455 (1996)
20. Y. Jia, S. Sun, S. Xue, L. Liu, G. Zhao, Polymer **44**, 319–326 (2002)
21. V. Kosar, Z. Gomzi, Thermochim. Acta **457**, 70–82 (2007)
22. ASTM D 5289-07. *Standard Test Methods for Vulcanized Rubber and Thermoplastic elastomers-tension*. Annual Book of ASTM Standards (2007)
23. A.V. Chapman, M. Porter, Sulfur vulcanization chemistry, in *Natural Rubber Science and Technology (Chap. XII)*, ed. by A.D. Roberts (Oxford University Press, Oxford, 1978)
24. M.R. Kresja, J.L. Koening, Rubber Chem. Technol. **66**, 376 (1993)
25. D.E. Goldberg, *Genetic Algorithms in Search, Optimization and Machine Learning* (Addison Wesley Publishing Company, Reading, MA, 1989)
26. R.B. Holstien, *Artificial Genetic Adaptation in Computer Control Systems*. Ph.D. Thesis, Department of Computer and Communication Sciences, University of Michigan, Ann Arbor, 1971
27. R.L. Haupt, S.E. Haupt, *Practical Genetic Algorithms* (Wiley, London, 2004)
28. Y. He, C.-W. Hui, Chem. Eng. Process. **43**(11), 1175–1191 (2007)
29. L. Montastruc, C. Azzaro-Pantel, L. Pibouleau, S. Domenech, Chem. Eng. Process. **43**(10), 1289–1298 (2004)
30. The Mathworks (Matlab 7.4 User's Guide Natick, MA ,2007), http://www.mathworks.com/products/matlab/
31. G. Natta, G. Crespi, G. Mazzanti, Ethylene-propylene copolymers containing unsaturations, in *Proceedings of 4th Rubber Technology Conference*, London, 1962
32. G. Natta, G. Crespi, G. Mazzanti, *L'industria della gomma [the rubber industry]*, 1 (1963)